Available online at www.sciencedirect.com
SCIENCE DIRECT®
Journal of Molecular Catalysis A: Chemical 228 (2005) 189–194
JOURNAL OF MOLECULAR CATALYSIS A: CHEMICAL
www.elsevier.com/locate/molcata

Catalytic effect of KOH on textural changes of carbon macro-networks by physical activation

J. Matos*, M. Labady, A. Albornoz, J. Laine, J.L. Brito

Laboratorio de Fisicoquímica de Superficies, Centro de Química, Instituto Venezolano de Investigaciones Científicas (I.V.I.C.), Apartado 21827, Caracas 1020-A, Venezuela

Available online 11 November 2004

Abstract

The synthesis and definition of the topological organization of polygonal macro-networks of carbon in the form of films have been performed by controlled pyrolysis of saccharose. The pentagon was found to be the most abundant polygon in the film networks, which presented ring areas in the range of 4–12 mm^2. In addition to the bi-dimensional films, irregular sponge balls were also obtained featuring a similar random network structure to that obtained in the films. The sponges developed into a continuous net of tri-dimensional random network in the form of tubes with coiled shapes. The formation of carbon macro-coils was attributed to the presence of potassium particles inside the original carbonaceous matrix. A study of textural changes of the macro-networks of carbon by activation under flow of N_2 and CO_2 has shown that it is possible to obtain activated carbons from the macro-networks with BET surface areas as high as 850 and 981 $m^2\,g^{-1}$ under flow of N_2 and CO_2, respectively. From the study of textural changes of the macro-networks of carbon, a detailed mechanism that involves the role of KOH as a catalyst for the activation of the macro-networks has been proposed.

Keywords: Carbon networks; Macro-coils; Physical activation; BET; KOH

1. Introduction

Cellular structures characterized by cells having areas and number of sides randomly distributed are commonly named networks [1,2]. Well defined, molecular networks such as fullerenes and nanotubes have been some of the most remarkable discoveries in the area of carbon research in recent years [3,4]. Another ill defined type of carbon network, is that corresponding to the microporous structure of activated carbons. Three types of carbonaceous network structures can be considered according to the size of cells: the molecular (fullerenes, nanotubes), the micro- (microporous carbon), and the macroporous carbon. Although in the case of carbon materials, synthetic routes for both molecular-networks and micro-networks have been extensively investigated [3,5], few studies exist regarding the synthesis and characterization of macro-networks [6]. This communication presents the synthesis and definition of the topological organization of two carbonaceous macro-network two-dimensional films obtained by a step-wise heat treatment of saccharose in presence or absence of potassium hydroxide and second, an experimental study of the textural changes of the carbonaceous network materials activated up to 800 °C with N_2 or CO_2.

2. Experimental

2.1. Network synthesis

Solutions composed of either 1 mL of water or 1 mL of aqueous solution (34 wt.%) of potassium hydroxide (Merck, analytical grade) plus 2 g of D(+)-saccharose (Merck, bacteriology grade) were placed inside 50 mL Pyrex beakers and stirred at 80 °C until a viscous and light brown solution was observed. Immediately, the solutions are left in rest until recrystallization of the saccharide, as a homogeneous and transparent plate in the bottom of the beaker. Then, the plates were submitted to two consecutive heat treatments. First, a

* Corresponding author. Tel.: +58 212 504 1922; fax: +58 212 504 1350.
E-mail address: jmatos@ivic.ve (J. Matos).

1381-1169/$ – see front matter © 2004 Elsevier B.V. All rights reserved.
doi:10.1016/j.molcata.2004.09.039

low temperature stabilization treatment inside an oven (static air) at 60, 90, 110, and 130 °C, for 10 min at each temperature using heating rates between steps of about 3 °C min^{-1}. The second heat treatment consists of carbonization under an inert flow of nitrogen (≅100 mL min^{-1}) using as step temperatures: 50, 100, 150, 200, 250, 350 °C, leaving 30 min at each temperature, and finally 1 h at 450 °C, using heating rates between steps of about 5 °C min^{-1}. The carbonaceous macro-network "blank" samples prepared as described above were denoted as A_{NW-1} and A_{NW-2}, respectively, for the saccharose dissolved in water or in KOH solution.

2.2. Statistical characterization of macro-network films

A statistical analysis of the macro-network films obtained was carried out as described in previous studies for other cell structural systems [1,2]. Several photographs of the films adhered to the beakers in two separated sets of A_{NW-1} and A_{NW-2} samples (each one by triplicate) were taken in order to carry out the statistical analysis of the film macro-networks, particularly the polygonal distribution of cells with n sides $\rho(n)$. A total of 750 and 558 cells were employed, respectively, for the analysis of A_{NW-1} and A_{NW-2} samples, and the error in measuring cell areas was less than 5%. In addition, for the macro-network films, the average polygonal areas $\langle A_n \rangle$, were estimated from data of n-sided polygon distributions.

2.3. Activation processing of the network

Besides the macro-network films, two types of carbonaceous three-dimensional networks were also obtained, that were employed for the study of textural changes by means of a activation processing. The activations were performed in a tubular furnace, under either inert N_2 flow (≅100 mL min^{-1}) at several final residence times: 5, 60, 120 and 300 min at constant final temperature of activation equal to 800 °C; or under CO_2 flow (≅100 mL min^{-1}) as a function of the final activation temperature: 700, 750 and 800 °C at constant residence time of 5 min.

2.4. Textural characterization of the networks

Textural characterization of the macro-network blanks and the activated network materials was performed by means of N_2 adsorption at 77 K in order to obtain the BET surface areas.

3. Results and discussion

3.1. Statistical analysis of macro-network films

In the two blanks (A_{NW-1} and A_{NW-2}) both two- and three-dimensional macro-networks were obtained simultaneously after carbonization. The macro-network films obtained were adhered both to the bottom and the cylindrical beaker walls,

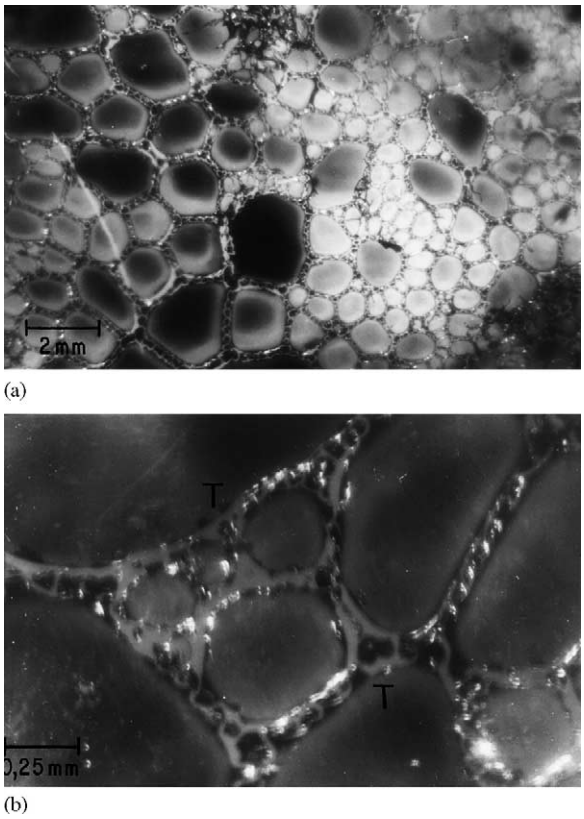

Fig. 1. Images of the carbonaceous macro-network film: (a) typical random pattern showing the predominance of five-sided cells; (b) a subsection showing the presence of "T" type vertices with internal angle $\theta = 180°$.

covering approximately one-third and one-half of the beaker height, respectively, for the A_{NW-1} and A_{NW-2} samples. For the case of bi-dimensional network, it consists of a random net of cells in the form of polygonal rings where each one is formed by grains of carbonaceous material. Polygons from three up to eight or nine sides were identified, respectively, for A_{NW-1} or A_{NW-2}, as can be seen in Fig. 1 specifically for A_{NW-2} network.

Fig. 2 shows the abundance of n-sided polygons ((n) obtained after the statistical analysis for A_{NW-1} and A_{NW-2} macro-network films. It can be noted from Fig. 2 that both

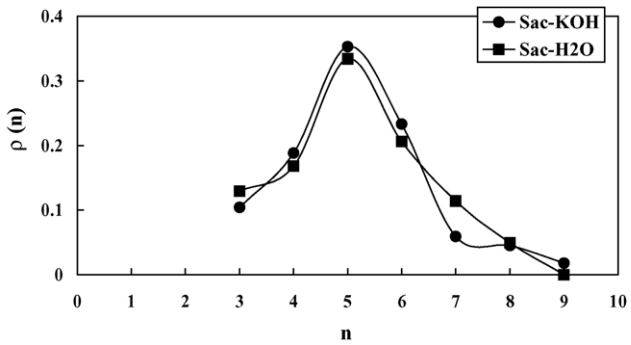

Fig. 2. Polygonal distributions in the macro-network A_{NW-1} (Sac-H_2O) and A_{NW-2} (Sac-KOH) films.

Table 1
Average polygonal areas $\langle A_n \rangle$ of the A_{NW-1} and A_{NW-2} macro-network films as function of the number of cell-sided

n-Sided cells	$\langle A_n \rangle$, A_{NW-1} (mm^2)	$\langle A_n \rangle$, A_{NW-2} (mm^2)
3	3.708	3.896
4	4.948	5.194
5	6.186	6.493
6	7.416	7.792
7	8.656	9.090
8	9.882	10.39
9	–[a]	11.69

[a] Polygonal cells of 9-sides were not detected in A_{NW-1} sample.

distributions are similar, showing that the pentagon is the most abundant polygon in the two macro-networks. Hence, from the experimental evidences shown in Fig. 2, the Euler topological relation [1,2] is modified according to:

$$\langle n \rangle_{A_{NW-1}} = \sum\nolimits_{n=3} [n \times \rho(n)] = 5.155 \quad (1)$$

$$\langle n \rangle_{A_{NW-2}} = \sum\nolimits_{n=3} [n \times \rho(n)] = 5.161 \quad (2)$$

respectively for A_{NW-1} and A_{NW-2} macro-network films.

Although this result has been obtained previously in microscopic polymer polygrain system [1,2], the present results are striking because in the existing literature regarding other macroscopic cell structural systems, the hexagon appears as the most abundant polygon. In addition, as can be seen in Table 1 most cell areas of the present networks fall inside the range 4–10 and 4–12 mm^2, respectively for the A_{NW-1} and A_{NW-2} carbonaceous films.

3.2. Morphological characteristics and chemical composition of the carbonaceous macro-network materials

As indicated above, in addition to the bi-dimensional films, irregular sponge-like balls were also obtained in the bottom of the beakers for the two samples. Images of bulk carbonaceous macro-network from the A_{NW-2} sample are shown in Fig. 3. It is interesting to remark that this three-dimensional feature [6,7] displays a similar random network structure than that obtained in the corresponding film (Fig. 1). Thus, the three-dimensional network shows a random structure characterized by a net of carbonaceous grains, whose topology has a form of polygonal cells with different sizes.

Also, a surprising morphological result was achieved [6]. Some of the carbonaceous cells that conform the macro-network present macro-coiled shapes (Fig. 3b). In the present case we attribute the formation of carbon macro-coils in the three-dimensional A_{NW-2} sample to the presence of potassium microparticles inside the carbonaceous matrix. This suggestion was indirectly confirmed by the fact that in case of the A_{NW-1} sponge (without the presence of potassium) the macro-coiled carbon filaments were not detected [7].

Since the present carbonaceous materials are a complex biphasic arrangement of crystalline lamellar and amorphous

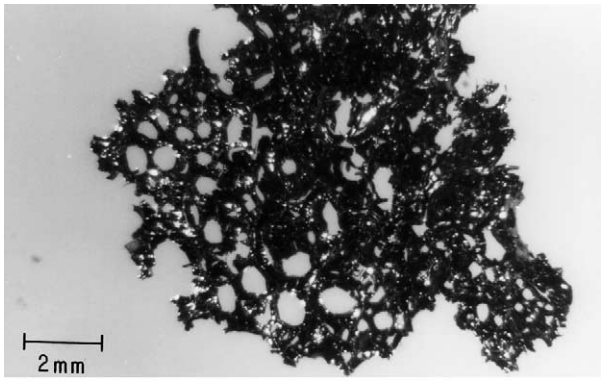

(a)

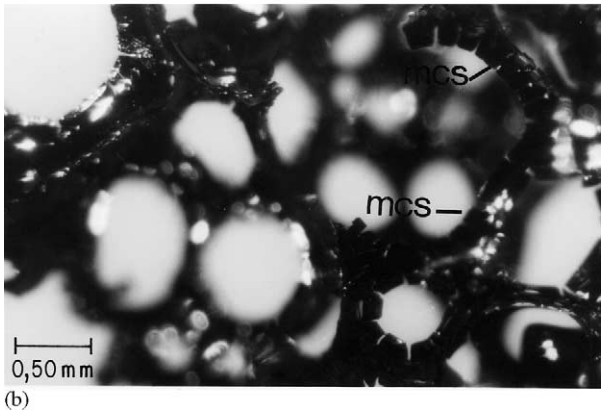

(b)

Fig. 3. Image of bulk carbonaceous macro-network from the A_{NW-2} sample: (a) three-dimensional random structure of a subsection of the sponge; (b) subsection showing macro-coil shapes (mcs).

phases, mainly of carbon, it is expected to evidence some topological changes due to possible discontinuities between crystalline–crystalline and crystalline–amorphous phases [2]. In particular, as the present networks are saccharose-based carbons, textural changes are expected during thermal activation experiments at temperatures higher than those employed for the carbonization [5,8].

3.3. Textural changes of the networks caused by activation

3.3.1. General discussion

To confirm this suggestion, activation studies with N_2 and CO_2 over the two types of three-dimensional bulk networks were carried out. Table 2 shows a summary of samples prepared and the experimental conditions employed. The BET surface areas of the A_{NW-1} and A_{NW-2} samples listed in Table 3 (10 and 15 $m^2\,g^{-1}$) suggest a non-porous texture in the present macro-networks of carbon. Also from Table 3, it can be seen that the burn-off was relatively high (about 85%) for A_{NW-1} with respect to those normally found after chemical activation (40–60%). However, the burn-off of the A_{NW-2} sample is only slightly higher than this range (about 66%). As can be seen also from Table 3, if the results of the A_{N2-2} and A_{CO2-2} samples are compared with those of

Table 2
Summary of experimental conditions employed for the study of textural changes of the carbonaceous macro-networks by activation with N_2 and CO_2

Networks	Activation temperature (°C)	Activation residence time (min)	Other experimental conditions
A_{N2-2}	800	60	N_2-activated from A_{NW-1}, without H_2O pre-washing
A_{CO2-2}	800	60	CO_2-activated from A_{NW-1}, without H_2O pre-washing
A_{N2-3}	800	60	N_2-activated from A_{NW-2}, with H_2O pre-washing
A_{CO2-3}	800	60	CO_2-activated from A_{NW-2}, with H_2O pre-washing
A_{N2-4A}	800	60	N_2-activated from A_{NW-2}, without H_2O pre-washing
A_{N2-4B}	800	120	N_2-activated from A_{NW-2}, without H_2O pre-washing
A_{N2-4C}	800	300	N_2-activated from A_{NW-2}, without H_2O pre-washing
A_{N2-4D}	800	5	N_2-activated from A_{NW-2}, without H_2O pre-washing
A_{CO2-4A}	800	60	CO_2-activated from A_{NW-2}, without H_2O pre-washing
A_{CO2-4B}	800	5	CO_2-activated from A_{NW-2}, without H_2O pre-washing
A_{CO2-4C}	750	5	CO_2-activated from A_{NW-2}, without H_2O pre-washing
A_{CO2-4D}	700	5	CO_2-activated from A_{NW-2}, without H_2O pre-washing

the A_{N2-3} and A_{CO2-3} samples, two interesting results arise. First, the total burn-off obtained on the A_{N2-2} and A_{CO2-2} samples are slightly higher (92 and 91%, respectively) than that obtained for the blank A_{NW-1} (85%). In addition, the total burn-off obtained for the A_{N2-3} and A_{CO2-3} samples are slightly higher (70 and 72%, respectively) than that obtained for A_{NW-2} (66%), yet they are only slightly higher than the range that normally is found in chemical activation processing. Second, it can be seen that for the case of the high oxidation process of activation with CO_2 (A_{CO2-2} sample) the BET surface area obtained from A_{NW-1} was moderate ($270\,m^2\,g^{-1}$) in comparison to the negligible surface area obtained for the case of activation with N_2 ($8\,m^2\,g^{-1}$). However, the BET surface areas obtained for the case of the A_{N2-3} and A_{CO2-3} samples show a different trend, the activation of A_{NW-2} under flow of N_2 (A_{N2-3}) promotes a higher BET surface area than that obtained for the A_{N2-2} sample obtained from A_{NW-1} (79 against $8\,m^2\,g^{-1}$), while for the activation under flow of CO_2, the A_{CO2-3} sample developed into a lower BET surface area than that obtained for the A_{CO2-2} sample (137 against $270\,m^2\,g^{-1}$). These changes in surface areas seem to indicate that although the A_{NW-2} sample was previously washed with H_2O (Table 2) there is still potassium remnant, probably in very low concentration but enough to inhibit an excessive pyrolysis and simultaneously to promote a higher BET surface area when the activation is undertaken over flow of nitrogen than that obtained from the physical activation of A_{NW-1} macro-network also under flow of N_2 ($79 \gg 8\,m^2\,g^{-1}$). Thus, the present results indicate that the KOH is an effective catalyst for the activation of the carbonized A_{NW-2} macro-network, both in presence of N_2 and specially CO_2.

Table 3
Total burn-off of saccharose and BET surface areas of the carbonaceous three-dimensional networks obtained

Networks	Saccharose burn-off[a] (%)	BET surface area ($m^2\,g^{-1}$)
A_{NW-1}	85	10
A_{NW-2}	66	15
A_{N2-2}	92	8
A_{CO2-2}	91	270
A_{N2-3}	70	79
A_{CO2-3}	72	137
A_{N2-4A}	72	558
A_{CO2-4A}	100	–[b]

[a] Except the corresponding values of A_{N2-3} and A_{CO2-3} that were previously washed with H_2O, all the rest of saccharose burn-off (%) values were estimated after subtracting the theoretical remnant weight of potassium as K_2O (≈0.4501 g).

[b] The BET surface area of the A_{CO2-4A} sample was not included since it was totally pyrolyzed.

The catalytic effect of the potassium is discussed as follows. It is well-known [9] that KOH at the surface of the carbonised lignocellulosic material is decomposed according to the reaction:

$$2KOH \rightarrow K_2O + H_2O \quad (3)$$

producing gaseous water that due to its small weight and molecular diameter can diffuse easily into the carbon porous structure, contributing to gasification. The basic reaction of carbon with water vapour is endothermic and of the following stoichiometry [10,11]:

$$H_2O + C \rightarrow CO + H_2,\ \Delta H = +117\,kJ\,mol^{-1} \quad (4)$$

In addition, products of Eq. (4) ($CO + H_2$), can be consumed by the abundant oxygen available from the carbonaceous matrix of the network [7]:

$$CO + H_2 + 2O \rightarrow CO_2 + H_2O \quad (5)$$

thus further increasing the concentrations of activators ($CO_2 + H_2O$).

Accordingly, the protection from excessive gasification found for the catalysis with potassium hydroxide could be the result of the formation of a layer of oxides (similarly to the layer of polyphosphate reported by Laine and Calafat [9]) over the developing porous structure, avoiding further interaction with gaseous CO_2 that would lead to excessive burn-off.

Similarly to the above gasification reaction (Eq. (4)), the reaction of carbon with carbon dioxide can be expressed as:

$$CO_2 + C \rightarrow 2CO,\ \Delta H = +159\,kJ\,mol^{-1} \quad (6)$$

On the other hand, as under practical conditions (above 800 °C) the water gas shift reaction is at equilibrium [11]:

$$CO + H_2O \rightleftarrows CO_2 + H_2 \quad (7)$$

Both reactions (4) and (6) are important despite the fact that in most cases superheated steam is the primary activation agent. However, this is not the present case, and therefore we suggest that the reactions (3–5) are the predominant steps occurring during the activation of the macro-networks with N_2, while the reactions (3–7) and particularly reactions (6) and (7) are all involved during the activation of the macro-networks with CO_2. The results listed in the last block of Table 3 are in line with the mechanism described above, which is based in the presence of potassium as KOH in order to initiate, by means of reaction (3), the catalytic activation effect over the carbonaceous network matrix. This effect is more remarkable for the sample activated under flow of CO_2 ($A_{CO2\text{-}4A}$) where the macro-network sample ($A_{NW\text{-}2}$) was totally pyrolyzed probably due to the increased presence of the activators ($CO_2 + H_2O$) produced according to the reaction (7).

3.3.2. Influence of the residence activation time

The results obtained are presented in Fig. 4 in terms of the BET surface areas and the total burn-off of saccharose that were estimated after subtracting the theoretical remnant weight of potassium as K_2O (≈0.4501 g). The burn-off shows a tendency to increase monotonically as a function of the residence activation time. The burn-off of the $A_{N2\text{-}4i}$ samples shown in Fig. 4 goes from 68% at 5 min to close to 80% at 300 min in agreement with the mechanism suggested before, principally by means of reactions (3–5). It is logical to think that the quantities of the activators ($CO_2 + H_2O$) produced from the reaction (5), are strongly increased at longer activation times leading to a higher activation of the carbonaceous matrix of the macro-network with their concomitant higher tendency to pyrolyze the saccharose. In terms of the BET surface areas developed for $A_{N2\text{-}4i}$ samples, it can be seen also from Fig. 4 that the macro-network ($A_{NW\text{-}2}$) suffers clear textural changes as a function of the residence time. It increases the surface area from 565 $m^2\ g^{-1}$ at 5 min ($A_{N2\text{-}4D}$) through a value of 558 $m^2\ g^{-1}$ at 60 min ($A_{N2\text{-}4A}$) up to a maximum value of 850 $m^2\ g^{-1}$ at 120 min ($A_{N2\text{-}4B}$); then it drastically falls down to 540 $m^2\ g^{-1}$ at 300 min ($A_{N2\text{-}4C}$). This result seems to indicate that with activation times higher than 2 h, the process of activation turns less efficient, probably due to the well-known effect of destruction of the fine microporous structure constituting the high surface area of L-type activated carbons [10].

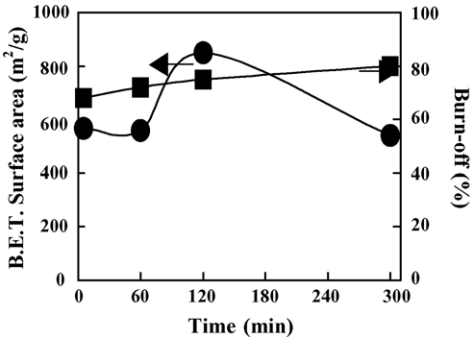

Fig. 4. Surface BET areas and burn-off behaviour of networks activated with N_2 (at 800 °C) as a function of residence time ($A_{N2\text{-}4i}$).

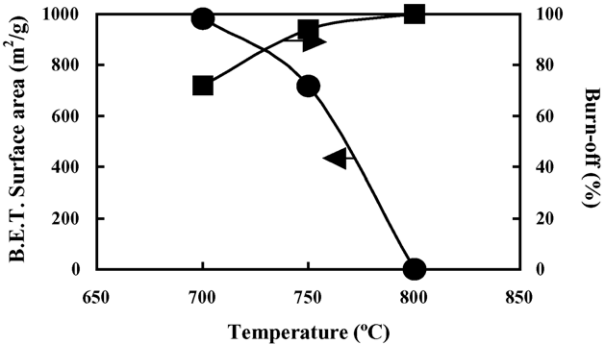

Fig. 5. Surface BET areas and burn-off behaviour of networks activated with CO_2 (by 5 min) as a function of the temperature ($A_{CO2\text{-}4i}$).

3.3.3. Influence of the activation temperature

These results are presented in Fig. 5 in terms of the BET surface areas and the total burn-off of saccharose. It can be seen from Fig. 5 that the burn-off shows a tendency to increase remarkably as a function of the activating temperature. The saccharose burn-off goes from a moderate value of 72% at 700 °C ($A_{CO2\text{-}4D}$) through a high value of 94% at 750 °C ($A_{CO2\text{-}4C}$) up to the maximum value of 100% at 800 °C ($A_{CO2\text{-}4D}$). This trend is in line with the mechanism suggested above by means of reactions (3–7). The most important steps of the mechanism correspond to the reactions represented by Eqs. (6) and (7), particularly the last one, which begins to be important when the temperature of activation approaches 800 °C. As can be seen in Fig. 5, the BET surface area values goes from 981 $m^2\ g^{-1}$ at 700 °C ($A_{CO2\text{-}4D}$) through 717 $m^2\ g^{-1}$ at 750 °C ($A_{CO2\text{-}4C}$) to fall down to cero when approaches 800 °C ($A_{CO2\text{-}4B}$) where the macro-network is totally pyrolyzed. This drastic textural change can be attributed to the fact that the microporous texture, obtained at the initial stages of the activation process, is destroyed in presence of strong oxidation conditions. In the present case, these conditions are favoured by both to the presence of potassium as KOH that produces H_2O by means of reaction (3), and also by high temperatures as indicates the reaction (7) because it promotes the production of CO_2. Therefore, from the results of Fig. 5 it can be suggested that in this case, it is occurring an accumulative effect of the highly oxidant agents: $H_2O + CO_2$, as indicate the reactions (3), (5), and mainly reaction (7). Both oxidant agents or activators (H_2O, and particularly CO_2) pyrolyze the carbona-

ceous matrix of the network by means of the two reactions of gasification (4) and (6).

4. Conclusions

Polygonal macro-networks in the form of films adhered to the bottom and walls of Pyrex flasks have been obtained by controlled pyrolysis of saccharose. The pentagon was found to be the most abundant polygon in the films, which presented ring areas in the range of 4–10 and 4–12 mm^2, respectively for the networks originated from saccharose pre-dissolved in water or in aqueous solution of 34 wt.% KOH.

In addition to the bi-dimensional films, irregular three-dimensional sponge balls featuring similar random network structures to that obtained in the films were obtained for the two samples prepared. These sponges are composed by an assembly of carbonaceous grains of different sizes with an interface where the carbon grains developed into a continuous net of three-dimensional random network in the form of macro-tubes with coiled shapes. The formation of carbon macro-coils was attributed to the presence of potassium microparticles inside the original carbonaceous matrix.

It is important to remark that with the activation process presented in the present work, activated carbons can be obtained with BET surface areas as high as 850 and 981 $m^2\,g^{-1}$ for the two different cases of activation with N_2 and CO_2, respectively. These values correspond to surface areas 85 and 98 times higher than that obtained on the non-activated macro-network of carbon. From this study a detailed mechanism that involves the role of the KOH as a catalyst for the activation of the macro-networks of carbon is proposed.

In the present, in order to better characterize such carbonaceous materials, we are performing a chemical surface analysis of these activated and non-activated macro-networks by means of X-ray photoelectronic spectroscopy.

References

[1] T. Huang, M.R. Kamal, A.D. Rey, J. Mater. Sci. Lett. 14 (1995) 220.
[2] M.R. Kamal, T. Huang, A.D. Rey, J. Mater. Sci. 32 (1997) 4085.
[3] H.W. Kroto, J.R. Heath, S.C. O'Brian, R.F. Curl, R.E. Smally, Nature 318 (1985) 162.
[4] M.R. Diehl, S.N. Yaliraki, R.A. Beckman, M. Barahona, J.R. Heath, Angew. Chem. Int. Ed. 41 (2002) 353.
[5] J.N. Rouzaud, A. Oberlin, Carbon 27 (1989) 517.
[6] J. Matos, M. Labady, A. Albornoz, J. Laine, J.L. Brito, J. Mater. Sci. 39 (2004) 3705.
[7] J. Matos, J. Laine, J. Mater. Sci. Lett. 17 (1998) 649.
[8] A. Burian, P. Daniel, S. Duber, J. Doré, Phil. Mag. B 81 (2001) 525.
[9] J. Laine, A. Calafat, Carbon 29 (1991) 949.
[10] J. Laine, S. Simoni, R. Calles, Chem. Eng. Commun. 99 (1991) 15.
[11] T. Wigmans, Carbon 27 (1989) 13.